Journal of Alloys and Compounds 513 (2012) 387–392

Contents lists available at SciVerse ScienceDirect

Journal of Alloys and Compounds

journal homepage: www.elsevier.com/locate/jallcom

Role of rare-earth elements in glass formation of Al–Ca–Ni amorphous alloys

Z.P. Chen, J.E. Gao, Y. Wu, H.X. Li, H. Wang, Z.P. Lu*

State Key Laboratory for Advanced Metals and Materials, University of Science and Technology Beijing, Beijing 100083, China

ARTICLE INFO

Article history:
Received 6 May 2011
Received in revised form 6 October 2011
Accepted 16 October 2011
Available online 25 October 2011

Keywords:
Glass forming-ability
RE elements
Atom size difference

ABSTRACT

Effects of different rare-earth (RE) elements (i.e., Y, Ce, La and Yb) on the glass forming-ability (GFA) of Al–Ca–Ni alloy system were systematically investigated. The optimum addition content of all the four RE is 1 at.% and ytterbium is the most effective as far as the GFA is considered. Our analysis confirmed that proper additions of Yb could not only impede the formation of the competing α-Al clusters, but also enhance the liquid stability (i.e., lower the liquidus temperature). Although additions of Y, Ce and La in the $Al_{88}Ca_7Ni_5$ can also retard the α-Al precipitation, nevertheless, it seemed that their large atomic size difference with Ca could destabilize the original liquid stability (i.e., increase the liquidus temperature).

1. Introduction

Al-based amorphous alloys have attracted extensive interest due to their unique combination of high specific strength and excellent corrosion resistance since they were discovered in 1988 [1–3]. Mechanical properties of Al-based metallic glasses can be further improved when nanoscale fcc-Al particles homogenously dispersed in the amorphous matrix, making them promising for light-weight engineering applications [4]. However, Al-based alloys have a relatively poor glass-forming ability (GFA) in comparison with the other light metal-based bulk metallic glasses (BMGs), such as Ca-based [5] and Mg-based BMGs [6]. Although serious efforts have been devoted to investigate the GFA of Al-rich amorphous alloy systems, nevertheless, the largest thickness for glass formation in Al-based alloy systems only reaches around 1 mm so far, as reported independently by Wang et al. [7] and Zhang et al. [8]. Thus, widespread uses of Al-based amorphous alloys have still been restricted because of their small critical size. Presently, most of the reported Al-based metallic glass systems typically contain 3–20 at.% RE (rare-earth) metal elements [9], which sacrifices the specific strength because of the high density of the RE elements. Therefore, it is necessary to understand further about glass formation in Al-based alloy systems and to explore potential good glass formers which contain limited contents of RE metals.

Alloying additions have been verified as an effective means for improving GFA in various BMGs [10,11], and actually, one of the best Al-based glass formers, i.e., the $Al_{86}Ni_7Y_{4.5}Co_1La_{1.5}$ alloy, was developed based on the $Al_{86}Ni_8Y_6$ base alloy via proper substitution of Ni and Y with Co and La elements [7], respectively. It is interestingly found that the Ca element has many similar properties with RE metals, including large atomic radius, low melting point and low Pauling's electronegativity. In this work, we attempt to develop new Al-based light-weight amorphous alloys based on the Al–Ca–Ni system [12]. It was found that minor substitution of Ca with RE elements in this alloy system can obviously increase the GFA. The roles of different RE metals (Y, Ce, La, Yb) on the GFA were also explored.

2. Experimental procedure

Elemental pieces (Al, Ni of 99.99% purity and Ca, La, Y, Ce, Yb of >99% purity) were used as starting materials. Master alloys with a nominal composition of $Al_{88}Ca_{7-x}Ni_5Yb_x$ (x = 0, 0.5, 1.5, 2, and 3 at.%) or $Al_{88}Ca_6Ni_5Re_1$ (Re = Y, Ce, La, Yb) were produced from the starting materials by arc-melting under a Ti-gettered argon atmosphere. 2 wt.% extra Ca was added to ensure consistence between the actual composition and nominal composition because of its volatility. To ensure the chemical homogeniety, all the ingots were melted at least four times. Wedge shaped specimens were obtained by injecting the alloy melt into a copper mold with a wedge cavity and as an example, Fig. 1 depicts the outer shape and surface appearance of the as-cast wedge samples of the $Al_{88}Ca_6Ni_5Yb_1$ and $Al_{88}Ca_7Ni_5$ alloys. Ribbon samples having a thickness about 40–70 μm and a width about 3–5 mm were prepared by remelting the alloys in a quartz tube and subsequently ejecting onto a copper wheel rotating with a surface velocity of 20 m/s. Structure of the ribbons and wedge specimens was investigated by X-ray diffraction (XRD) using Cu Kα radiation and high resolution transmission electron microscopy (HRTEM). The wedge specimens were grinded and polished, then etched about 10 s using a modified Keller's reagent (i.e., 4 ml HNO_3, 2.5 ml HCl, 1.5 ml HF and 200 ml distilled water). The TEM samples were first mechanically ground to a 50 μm thick and then twin-jet electropolished using a solution mixed in the ratio $HClO_4$:C_2H_5OH = 1:19. The critical dimension for glass formation of the wedge samples was examined by scanning electron microscopy

* Corresponding author. Tel.: +86 10 82375387; fax: +86 10 62333447.
E-mail address: luzp@ustb.edu.cn (Z.P. Lu).

0925-8388/$ – see front matter © 2011 Elsevier B.V. All rights reserved.
doi:10.1016/j.jallcom.2011.10.054

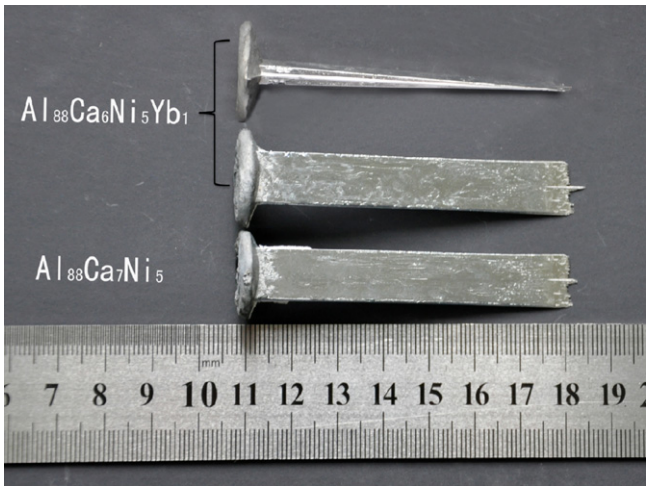

Fig. 1. The outer shape and surface appearance of the as-cast wedge samples of the $Al_{88}Ca_6Ni_5Yb_1$ and $Al_{88}Ca_7Ni_5$ alloys.

(SEM). Crystallization behavior of all ribbons was studied by differential scanning calorimetry (DSC) at a heating rate of 20 K/min.

3. Results

Fig. 2 shows the XRD patterns of the as-spun $Al_{88}Ca_{7-x}Ni_5Yb_x$ (x = 0, 0.5, 1, 1.5, 2, and 3.0 at.%) alloys. For the alloys containing 0–2% Yb, only a diffuse broad peak is observed, suggesting that the alloys have a mostly amorphous structure. For the alloy with 3 at.% Yb, however, sharp crystalline peaks which correspond to the α-Al, $CaNiAl_9$ and AlNiYb phase, indicating that the GFA are reduced due to the excessive Yb addition. To further determine the optimum Yb substitution content, wedge-casting of all the Yb-containing alloys has conducted. The wedge samples were first etched about 10 s using the modified Keller's reagent, and Figs. 3 and 4 show representative SEM images of the wedge-shaped samples of the $Al_{88}Ca_7Ni_5$ and $Al_{88}Ca_6Ni_5Yb_1$ alloys, respectively. For the base ternary alloy, a clear transition in the microstructure at the sample width of 280 μm is observed. The blowups of the regions A and B shown in Fig. 3b and c suggests that no any amorphous phase forms and the structure changes from fine equiaxed crystals to coarse dendrites. With 1% Yb substitution, the structure transition occurs

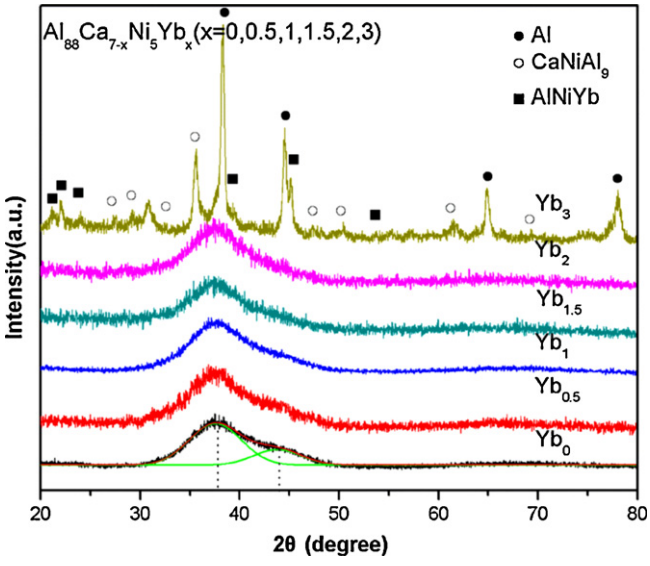

Fig. 2. XRD patterns of the as-spun $Al_{88}Ca_{7-x}Ni_5Yb_x$ (x = 0, 0.5, 1, 1.5, 2, 3) alloys.

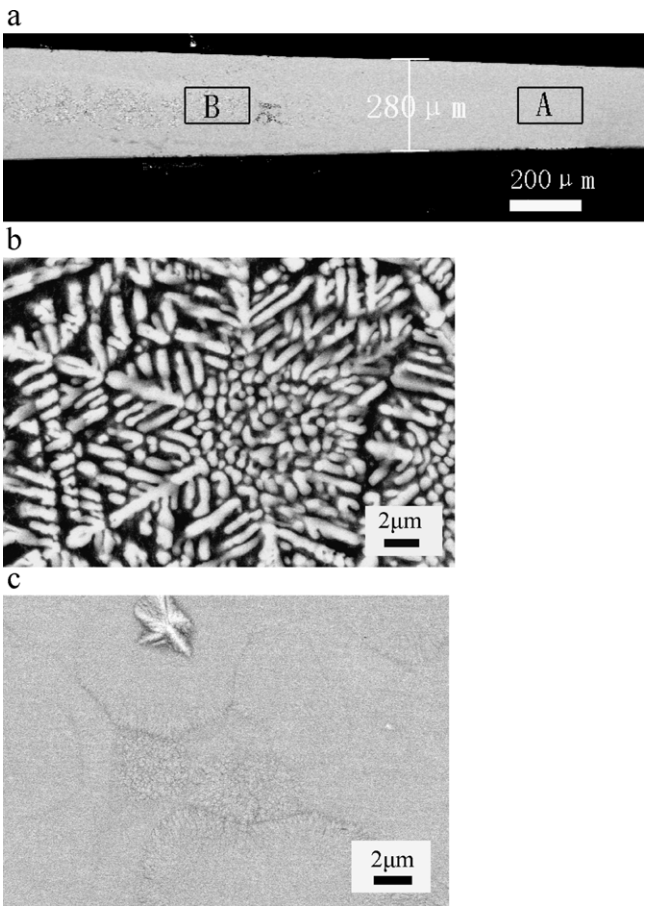

Fig. 3. SEM images of the $Al_{88}Ca_7Ni_5$ alloy; (a) macrostructure of the wedge-cast sample etched by the modified Keller's reagent, (b) the amplified image of the region B shows the coarse dendrites and (c) the amplified image of the region A shows the fine equiaxed crystals.

at the width of 370 μm. Enlarged images of the A and B regions in Fig. 4a imply that the region A has a fully amorphous structure while the region B is fully crystalline, suggesting that the critical thickness for glass formation (i.e., the maximum attainable thickness of the specimen with a fully amorphous structure) in this alloy is around 370 μm. Fig. 4d shows the corresponding DSC curves of regions A and B region, respectively. Sample from the region A shows clearly exothermic peaks associated with the crystallization event, while sample B exhibit nothing but a straight line, which are consistent with the SEM observations. The critical thickness for glass formation D_c as a function of Yb content is listed in Table 1. As shown, the best GFA has been achieved in the alloy containing 1 at.% Yb.

Similar wedge-casting experiments were carried out for the substitution with the other RE elements La, Ce and Y in the base ternary alloy. It was found that for all the RE elements investigated, the optimum doping amount is around 1 at.%. The critical thickness for glass formation in the alloys doped with 1 at.% La, Ce and Y is determined

Table 1
Thermal properties, GFA parameter γ and the critical thickness of the $Al_{88}Ca_{7-x}Ni_5Yb_x$ (x = 0, 0.5, 1, 1.5, 2, 3) alloys.

Alloys	T_{x1} (K)	T_m (K)	T_L (K)	$\gamma = T_x/(T_x + T_L)$	D_c (μm)
$Al_{88}Ca_7Ni_5$	431	881	983	0.305	70
$Al_{88}Ca_{6.5}Ni_5Yb_{0.5}$	439	872	976	0.31	70
$Al_{88}Ca_6Ni_5Yb_1$	444	872	971	0.314	370
$Al_{88}Ca_{5.5}Ni_5Yb_{1.5}$	441	872	1031	0.3	330
$Al_{88}Ca_5Ni_5Yb_2$	442	872	1039	0.298	270
$Al_{88}Ca_4Ni_5Yb_3$	–	875	1050	–	–

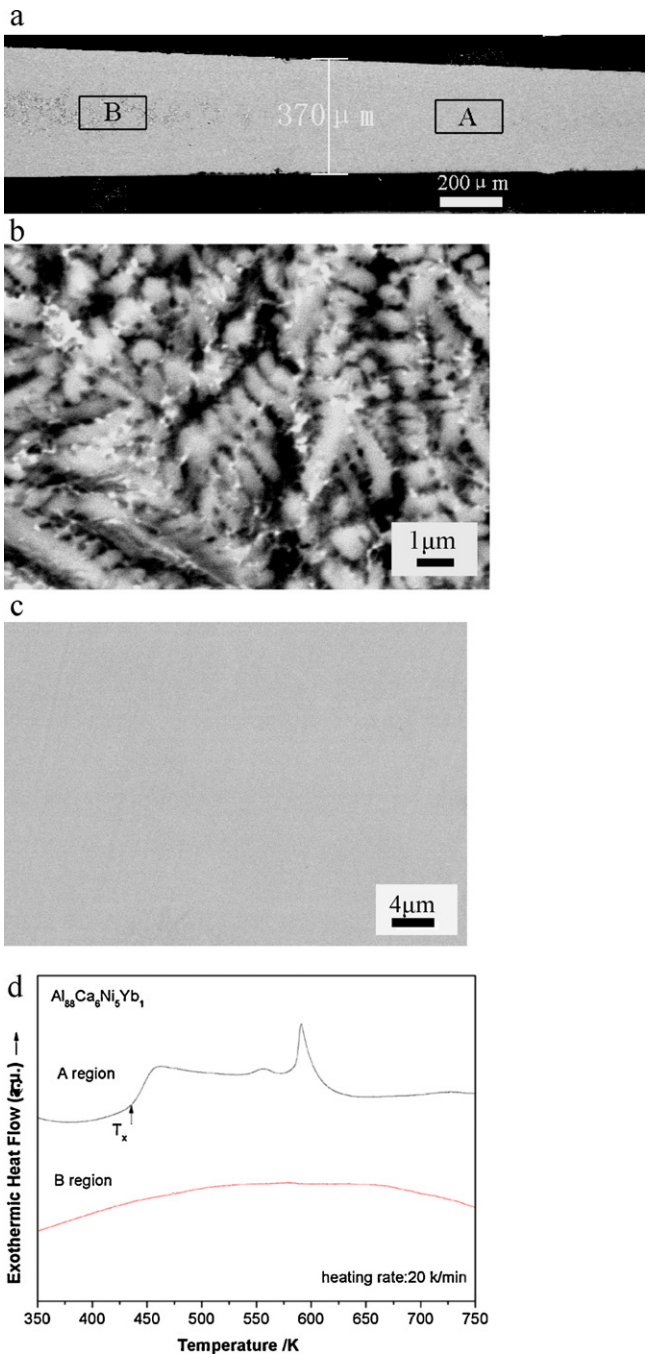

Fig. 4. SEM images and DSC curves of the $Al_{88}Ca_6Ni_5Yb_1$ alloy; (a) macrostructure of the wedge-cast sample etched by the modified Keller's reagent, (b) the amplified image of the region B shows the coarse dendrites (c) the amplified image of the region A shows the amorphous structure, and (d) DSC curves of regions A and B, respectively.

to be 310, 290 and 260 μm, respectively (see Table 2). Clearly, ytterbium is the most effective in enhancing the GFA of the base ternary Al–Ca–Ni alloy.

4. Discussion

4.1. Effect of the Yb substitution on glass formation

For understanding effect of the Yb substitution on glass formation, DSC measurement of crystallization and melting behavior of the as-spun ribbons were characterized at a heating rate of 20 K/min and the corresponding results are shown in Fig. 5. Thermal parameters of these alloys, including T_x (the onset crystallization temperature), T_m (the onset melting temperature), T_L (the liquidus temperature) and the GFA parameter γ (T_g was replaced by T_x in the original equation because the glass transition temperature has not been detected [13]) are tabulated in Table 1. As shown, the γ value of all the Yb-containing alloys is less than 0.35, suggesting that these alloys are still not bulk glass formers [14]. Next, the beneficial effect of the Yb additions on the GFA is discussed from the frame work of crystalline resistance and liquid phase stability.

In the base alloy, the main competing crystalline phase is α-Al. Additions of Yb can retard the formation of nanocrystalline α-Al and enhance crystallization resistance of the supercooled

Table 2
Thermal properties, GFA parameter γ and the critical thickness of the $Al_{88}Ca_6Ni_5X_1$ (X = Y, Ce, La and Yb) alloys.

Alloys	T_{x1} (K)	T_m (K)	T_L (K)	$\gamma = T_x/(T_x + T_L)$	D_c (μm)
$Al_{88}Ca_6Ni_5Y_1$	445	876	1077	0.292	260
$Al_{88}Ca_6Ni_5Ce_1$	447	877	994	0.31	290
$Al_{88}Ca_6Ni_5La_1$	458	878	1012	0.312	310
$Al_{88}Ca_6Ni_5Yb_1$	444	872	971	0.314	370

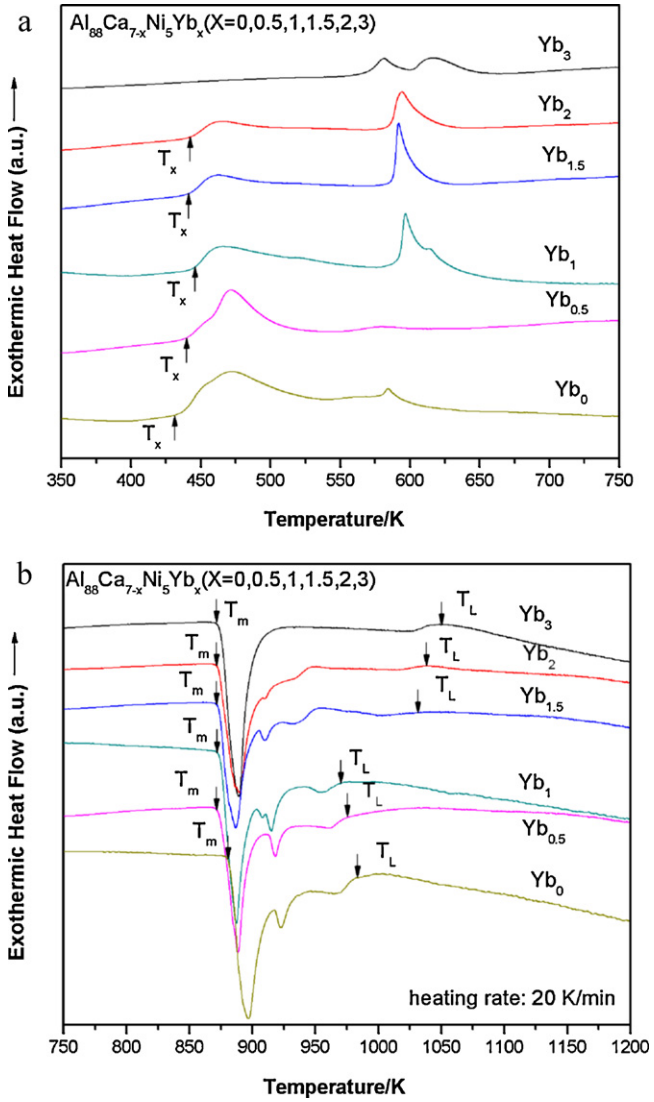

Fig. 5. DSC curves of the as-spun $Al_{88}Ca_{7-x}Ni_5Yb_x$ (x = 0, 0.5, 1, 1.5, 2, 3 at.%) alloys at a heating rate of 20 K/min.

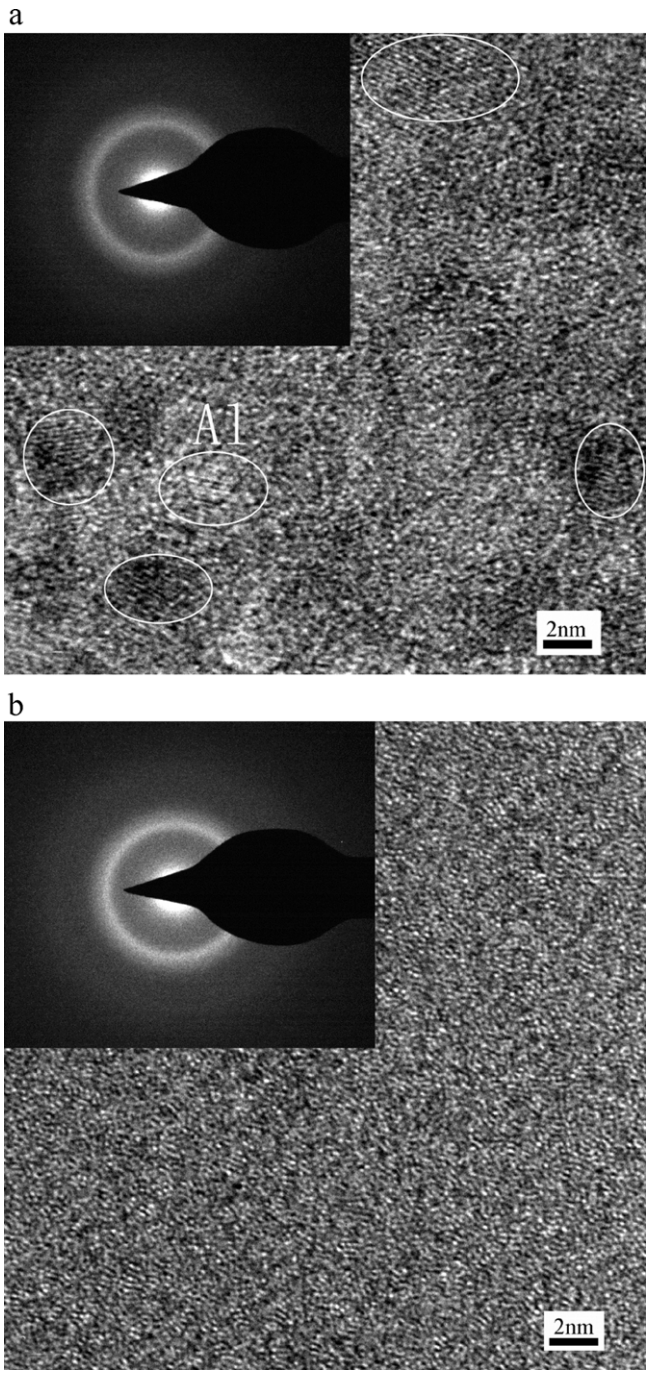

Fig. 6. HRTEM images of the as-spun $Al_{88}Ca_7Ni_5$ (a) and $Al_{88}Ca_6Ni_5Yb_1$ ribbon (b). The inset in each image is the corresponding SAED pattern, and white circles in (a) indicate quenched-in α-Al clusters.

liquids as shown in Fig. 2, the XRD trace of the as-spun base ternary $Al_{88}Ca_7Ni_5$ alloy (i.e., Yb = 0 at.%) shows a diffuse halo together with a faint additional shoulder at about $2\theta = 44^\circ$. Such shoulder is unusual for a fully amorphous structure, but seems to be a typical characteristic of the Al-based glassy systems [12], as also observed in the quenched $(Al_{75}Cu_{17}Mg_8)_{97}Ni_3$ and $Al_{85}Ni_5Y_6Co_2Pd_2$ alloys [15,16]. We have used the Gaussian multiple function to fit the double-peak and found that the weak shoulder is seemingly associated with quenching-in α-Al nanosized clusters in the as-spun $Al_{88}Ca_7Ni_5$ alloy ribbon. In order to confirm this conjecture, HRTEM observation of the as-spun $Al_{88}Ca_7Ni_5$ ribbons and the corresponding result are presented in Fig. 6a. As shown in this figure,

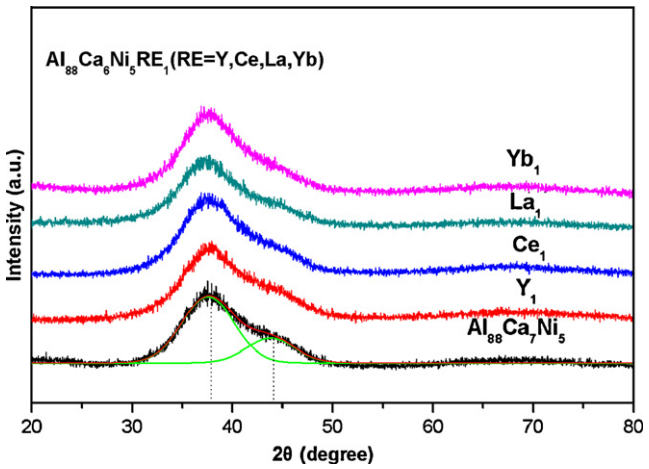

Fig. 7. XRD patterns of the as-spun $Al_{88}Ca_6Ni_5X_1$ (X = Y, Ce, La and Yb) alloys.

quenched-in α-Al nuclei do exist in the glass matrix of the base alloy and their size is in the range of about 3–6 nm (Fig. 6a), confirming that the additional shoulder on the XRD trace was caused by the small α-Al clusters. Nevertheless, the selected area electron diffraction (SAED) pattern is still typical for glass alloys, which is probably due to the fact that the volume fraction of these quenched-in α-Al nuclei is lower than the XRD detection limit. When 1 at.% Ca was replaced by the Yb element, the additional shoulder became almost invisible (Fig. 2). Compared with the base $Al_{88}Ca_7Ni_5$ sample, the HRTEM image of the as-spun $Al_{88}Ca_6Ni_5Yb_1$ alloy (Fig. 6b) shows a homogeneous featureless contrast and the SAED pattern is typical for amorphous alloys, verifying that the formation of quenching-in nanosized α-Al has been suppressed due to Yb additions. In addition, it can be seen from Table 1 and Fig. 5a that, with the increase of Yb, the onset crystallization temperature is initially increased and reaches the maximum of 444 K in the alloy with 1 at.% Yb, further confirming that proper substitution of Ca with Yb can suppress the formation of α-Al and enhance crystallization resistance, i.e., improve the GFA.

In addition, based on Fig. 5b and Table 1, the liquidus temperature of the base $Al_{88}Ca_7Ni_5$ alloy is around 983 K. As calcium is replaced by Yb in the alloy, the liquidus temperature gradually decreases and shows a minimum value of 971 K in the alloy with 1 at.% Yb. Nevertheless, excessive substitution (more than 1 at.%) of Yb results in formation of another new AlNiYb phase and leads to increment in the liquidus temperature. All these observations imply that adequate Yb substitution can increase the liquid phase stability and thereby favor glass formation.

4.2. *Effects of different RE elements on glass formation*

Chemically, the four RE elements are similar to each other, such as large atomic radius and low Pauling's electronegativity. However, their effects on glass formation are varied, as demonstrated by the critical thickness shown in Table 2. The roles of different RE elements can be fully understood from Figs. 7 and 8 which show the XRD patterns and the DSC measurements of the alloys doped with 1 at.% Y, Ce, La and Yb, respectively. As shown in Fig. 7, the splitting shoulder on the main halo of the base alloy is depressed to a different degree with additions of the RE elements and become almost invisible in the Yb-containing alloy. Moreover, the onset crystallization temperature of all the alloys doped with 1 at.% RE is higher than that of the base $Al_{88}Ca_7Ni_5$ alloy. All these facts indicate that addition of 1 at.% RE metals favors glass formation due to the suppression of competing crystalline phases.

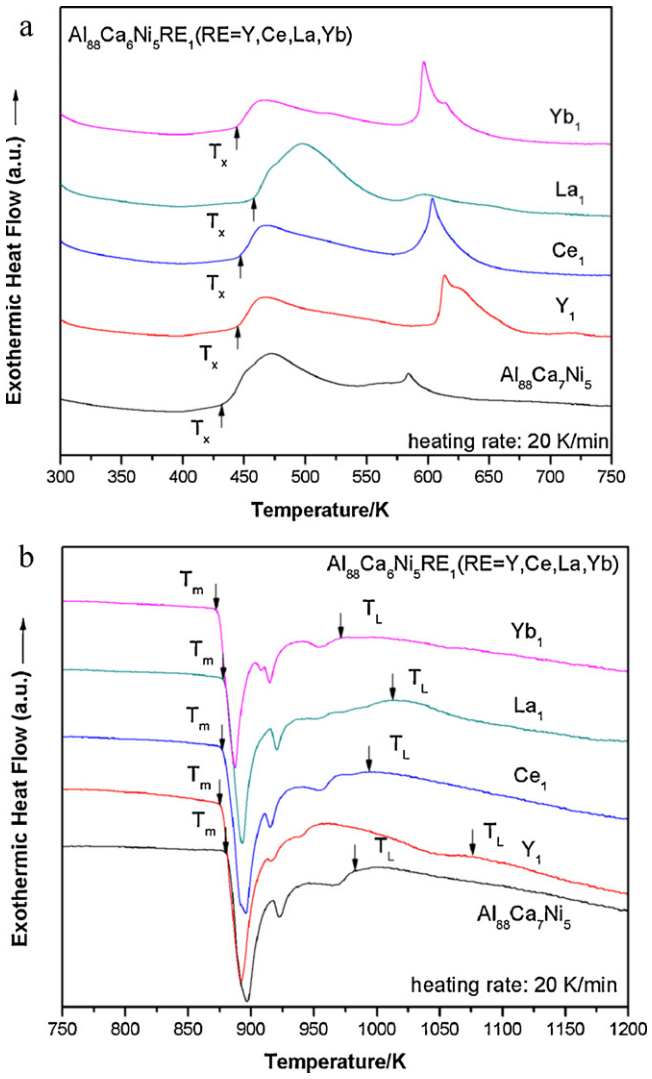

Fig. 8. DSC curves of the $Al_{88}Ca_7Ni_5$ and $Al_{88}Ca_6Ni_5X_1$ (X = Y, Ce, La and Yb) samples at a heating rate of 20 K/min.

On the other hand, the liquidus temperature is 994, 1012 and 1077 K for the addition of 1 at.% Ce, La and Y, respectively, but decreases to 971 K in the alloy doped with 1 at.% Yb (Table 2). Compared with that of the base alloy (i.e., 983 K), the liquidus temperature actually increased with the addition of 1 at.% RE elements, except for the alloy with 1 at.% Yb substitution. As such, additions of Y, Ce and La would destabilize the liquid stability and disfavor the glass formation. Such difference in the liquid phase stability could associate with the atomic size difference between the RE elements and Ca, as demonstrated in Fig. 9 which shows the critical thickness for glass formation as a function of the atomic size difference between the doping RE metal and Ca. The atomic size of all the four RE elements is in the order of Y (1.80 Å) < Ce (1.82 Å) < La (1.83 Å) < Yb (1.93 Å) [17]. Ytterbium is chemically similar to the RE elements Y, Ce and La, but has much closer atomic size with Ca (i.e., 1.97 Å). Although minor additions of all the aforementioned RE elements can suppress the formation of α-Al clusters, only would the Yb element retain the original densely packed topological structure in the base alloy. Substituting Ca with Y, Ce and La would lower or destroy the highly packed atomic structure due to the large atomic size difference between Ca and the RE element. Consequently, the liquid phase is destabilized and the liquidus temperature is thus increased, as depicted in Fig. 9.

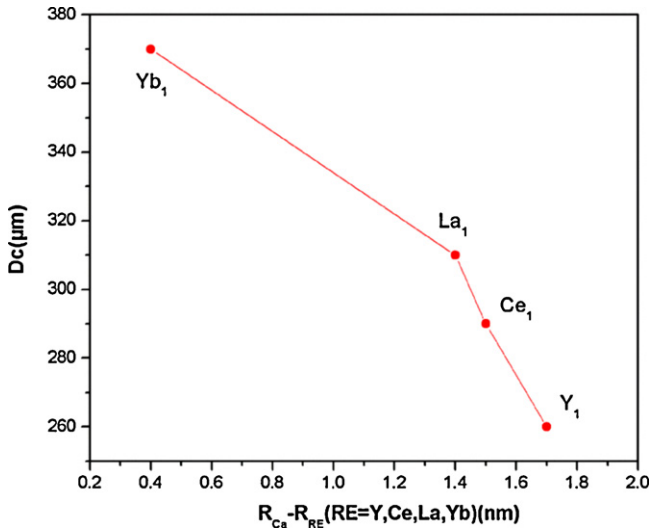

Fig. 9. The relation between D_c and atomic size difference between Ca and the RE element ($R_{Ca} - R_{RE}$) in $Al_{88}Ca_6Ni_5X_1$ (X = Y, Ce, La and Yb) alloys.

Glass formation is an intricate and complex metallurgical phenomenon and both crystallization resistance and liquid phase stability play important roles in the overall GFA [18]. Since all the four RE elements have large similarity in chemical properties, the difference in the liquid stability arisen from the atomic size difference may explain why among the four RE elements, the Yb element is the most effective in enhancing the GFA. Indeed, the critical thickness for glass formation is proportional to the atomic size difference between Ca and the doped RE metal (i.e., $R_{Ca} - R_{RE}$), as shown in Fig. 9.

5. Conclusions

(1) For the Yb-doped alloys, the optimum doping content is 1 at.% Yb. Proper Yb additions can not only suppress the formation of α-Al clusters (i.e., increase the crystallization resistance) but also enhance the liquid phase stability (i.e., lower the liquidus temperature), leading to the enhancement in the GFA.
(2) For all the four RE elements, ytterbium is the most effective in improving GFA of the Al–Ca–Ni alloy. Although additions of all the RE elements could impede precipitation of formation of α-Al clusters, only Yb can retain the original densely packing structure due to its smallest atomic size difference with Ca and enhance the liquid phase stability (i.e., a lowest liquidus temperature).

Acknowledgements

This work was supported by National Basic Research Program of China (973 program) under the contract 2007CB613903 and National Natural Science Foundation of China under the contract 50725104.

References

[1] Y. He, S.J. Poon, G.J. Shiflet, Science 241 (1988) 1640–1642.
[2] A. Inoue, K. Ohtera, A.P. Tsai, T. Masumoto, Jpn. J. Appl. Phys. 27 (1988) L280–L282.
[3] A.P. Tsai, A. Inoue, T. Masumoto, Metall. Trans. A 19 (1988) 391–393.
[4] Y.H. Kim, A. Inoue, T. Masumoto, Mater. Trans. JIM 31 (1990) 747–749.
[5] O.N. Senkov, D.B. Miracle, V. Keppens, P.K. Liaw, Metall. Mater. Trans. A 39 (2008) 1891–1892.
[6] H. Ma, L.L. Shi, J. Xu, Y. Li, E. Ma, Appl. Phys. Lett. 87 (2005) 181915.
[7] B.J. Yang, J.H. Yao, J. Zhang, H.W. Yang, J.Q. Wang, E. Ma, Scripta Mater. 61 (2009) 423–426.

[8] L.C. Zhuo, S.J. Pang, H. Wang, T. Zhang, Chin. Phys. Lett. 26 (2009) 066402.
[9] H. Yang, J.Q. Wang, Y. Li, J. Non-cryst. Solids 354 (2008) 3473–3479.
[10] Z.P. Lu, C.T. Liu, C.A. Carmichael, W.D. Porter, J. Mater. Res. 19 (2004) 921–929.
[11] W.H. Wang, Progr. Mater. Sci. 52 (2007) 540–596.
[12] J.D. Ayers, H.N. Jones, C.L. Vold, Scripta Met. Mater. 29 (1993) 205–209.
[13] Z.P. Lu, C.T. Liu, Acta Mater. 50 (2002) 3501–3512.
[14] Z.P. Lu, H. Bei, C.T. Liu, Intermetallics 15 (2007) 618–624.
[15] F.Q. Guo, S.J. Enouf, S.J. Poon, Philos. Mag. Lett. 81 (2001) 203–211.
[16] D.V. Louzguine, A. Inoue, J. Alloys Compd. 399 (2005) 78–85.
[17] J.G. Speight, Lange's Handbook of Chemistry, 16th ed., McGraw-Hill, New York, 2005, pp. 1151–1156.
[18] Z.P. Lu, C.T. Liu, Phys. Rev. Lett. 91 (2003) 115505.